

# A Dimerization Hierarchy in the Transmembrane Domains of the HER Receptor Family<sup>†</sup>

Jean-Pierre Duneau,<sup>\*,‡</sup> Attila P. Vegh,<sup>‡,§</sup> and James N. Sturgis<sup>‡</sup>

*Unité Propre de Recherche-9027 Laboratoire d'Ingénierie des Systèmes Macromoléculaires, Institut de Biologie Structurale et Microbiologie, Centre National de la Recherche Scientifique, 31 Chemin Joseph Aiguier, 13402 Marseille Cedex 20, France, and Institute of Biophysics and Radiation Biology, Faculty of Medicine, Semmelweis University, H-1088, Puskin u. 9, Budapest, Hungary*

*Received July 16, 2006; Revised Manuscript Received October 6, 2006*

**ABSTRACT:** Bitopic membrane proteins offer an opportunity for studying transmembrane domain interactions without the structural complexity inherent to multitopic integral membrane proteins. To date, only homomeric associations have been extensively studied quantitatively. Here we propose to assess the thermodynamics of heteromeric associations, which opens the way to investigating specificity and selectivity. A very interesting system of biological relevance with single transmembrane domains possibly involved in interactions with different partners is the EGFR receptor family. The four members, all tyrosine kinase receptors, are involved in an interaction network that potentially leads to a complete set of homo- and heterodimers, ideally suited to such a study. Furthermore, the transmembrane domains of these receptors have been previously implicated in their function in the past by mutations in the transmembrane domain leading to constitutive activation. We demonstrate, using a fluorescence-based measurement of interaction energies, a hierarchy of transmembrane domain interactions ranging from a noninteractive pair to strong dimerization. We propose a structural model based on the crystal structure of the EGFR dimer, to show how the dimeric structure favors these interactions. The correlation we observe between transmembrane domain and whole receptor interaction hierarchies opens a new perspective, suggesting a role for transmembrane receptor domains in the modulation of receptor signaling.

The association of transmembrane helices plays an important role both in the assembly and in the function of membrane proteins (1, 2). In the case of polytopic membrane proteins, the precise evaluation of these interactions is often obscured by their complex architecture that also involves prosthetic groups (3), extramembrane loops (4), membrane-adsorbed helices (5), and other peri- and extramembraneous elements (6).

Thus, many studies on the association of bitopic membrane proteins, particularly glycophorin A, have been performed to gain insight into the assembly of membrane proteins (7).

For example, such studies show that certain sequence motifs in transmembrane helices are responsible for the homodimeric structure of glycophorin A (8, 9). The GlyXXXGly motif (X is any residue) gives rise to a groove on one face of the helix which allows the close approach of the two helices, thus maximizing packing along the length of the two helices. Several large-scale studies of membrane proteins, both of their sequences (10, 11) and of structures (12, 13), have shown that this motif could be extended to a SmXXXSm sequence (Sm corresponds to small residues Gly,

Ala, Ser, or even Thr and X is any residue). This has been supported by biochemical investigations of designed sequences (14). This motif is, however, very common, giving rise to a huge number of potential oligomerization motifs in transmembrane helices.

To date, quantitative studies of transmembrane helix association have largely concentrated on homodimer formation (15–17); however, the majority of transmembrane helix associations are heterologous in both the assembly and function of integral membrane protein. This situation has been largely driven by experimental constraints. These constraints can, however, be overcome and measurement extended to heteromeric associations (18), allowing insights relevant for polytopic membrane protein folding and function.

In the work we report here we have used the HER<sup>1</sup> family of receptor tyrosine kinases as a model system. This family has four members, including the epidermal growth factor receptor (EGFR), HER2, HER3, and HER4.

A major feature of this family is its position in a cellular interaction network that can promote cell proliferation, differentiation, motility or apoptosis, and growth arrest (19).

<sup>†</sup> Supported by CNRS and La Ligue Contre le Cancer. A.P.V. was supported by a Marie Curie Fellowship from the European Union.

<sup>\*</sup> To whom correspondence should be addressed: UPR9027, LISM/CNRS, 31 Chemin Joseph Aiguier, 13402 Marseille Cedex 20, France. Telephone: 00 33 4 911 644 85. Fax: 00 33 4 917 121 24. E-mail: duneau@ibsm.cnrs-mrs.fr.

<sup>‡</sup> Centre National de la Recherche Scientifique.

<sup>§</sup> Semmelweis University.

<sup>1</sup> Abbreviations: HER, human Egfr related receptor; EGFR, epidermal growth factor receptor; FGFR3, fibroblast growth factor receptor 3; FRET, fluorescence resonance energy transfer; tm, transmembrane; Sm, small residues; ECD, extracellular domain; LDAO, *N,N*-dimethyl-*n*-dodecylamine *N*-oxide; TFA, trifluoroacetic acid; HOAt, 1-hydroxy-7-azabenzotriazole; HATU, *O*-(7-azabenzotriazolyl)-1,1,3,3-tetramethyluronium hexafluorophosphate; CD, circular dichroism; TFE, trifluoroethanol.

HER1tm *K642* **IP****SIAT****TGM****VGALL****LLLV****VAL****GIGL****YMR****RRH***672*  
 HER2tm *M546* **SN****LT****SI****IS****SA****VGILL****VVVL****GVV****YGILI****KRR***Q679*  
 HER3tm *K639* **THL****TMA****LT****VIAG****LVVIF****MM****LG****TFL****YH****GR***R670*  
 HER4tm *R649* **TL****PIA****AG****VIG****GLF****LIV****VL****TF****AVY****VRR****KS***679*

FIGURE 1: Sequences of the synthesized transmembrane domains. Proposed N- and C-terminal juxtamembrane residues are shown in italics. Putative SmXXXSm (see the text) interaction sites are underlined. Polar S and T residues that may be involved in interfacial hydrogen bonding are represented in boldface. Boxed residues correspond to modifications to the human sequence that were introduced to facilitate measurements (see Materials and Methods). The sequence numbering corresponds to the Swiss-Prot annotation of the human receptors (P00533, P04626, P21860, and Q15303).

This network associates a dozen or so ligands in different patterns of receptor association that drive cellular responses (19–21).

The first evidence of a role for the transmembrane helix in the function of these receptors came from the observation that a single hydrophobic to polar mutation within this domain of HER2/neu is associated in rat with chemically induced glioma- and neuroblastomas (22). It was shown that the mutation constitutively activates the receptor by oligomerization (23). The transmembrane domains of HER receptors exhibit several SmXXXSm motifs (24, 25) (Figure 1), and their involvement in the receptor function has frequently been questioned. A bacterial genetic assay (TOX-CAT) has shown that the four transmembrane domains are able to form homodimers (26), and further peptides corresponding to the transmembrane sequences can specifically inhibit the receptors in vivo (HER2/neu) (27) and in vitro (EGFR and HER2) (28, 29). Furthermore, this network gives a relatively restrained number of biologically relevant homo- and heterodimers.

To address these considerations, the dissociation constants for the four different homologous and six heterologous pairs of transmembrane helices were accurately measured using a well-controlled assay. A wide range of apparent dissociation constants were observed in a fixed micellar environment. Thus, transmembrane domains, even if greatly enriched in hydrophobic residues, and with reduced sequence complexity, can govern a complex hierarchy of interactions. To examine whether the crystal structure of the dimeric EGFR extracellular domain (ECD) is compatible with an energetic contribution from the transmembrane helices, we have built a model for a membrane-associated receptor.

In view of the similarity of our results with the literature on whole receptor behavior, and in particular the correlation between the transmembrane domain and whole receptor association preferences, we suggest that the observed hierarchy of transmembrane domain dimerization may play a role in both the strength of the interactions between activated receptors and the specificity and selectivity of these interactions.

## MATERIALS AND METHODS

**Design of the Transmembrane Domain Sequences.** The sequences that were synthesized (Figure 1) contain several minor changes to facilitate our measurements. In EGFRtm and HER2tm, a Phe was replaced with a Tyr, to aid detection

of unlabeled peptides. For HER2tm, the N-terminal juxtamembrane sequence, the native Ala-Ser-Pro sequence, was modified to a Met-Ser-Asn sequence, due to requirements for other experiments. In the HER3tm sequence, the Trp was replaced with a His, as found in the sequence of *Fugu rubripes*, to prevent problems due to Trp–coumarin fluorescence energy transfer.

**Reagents.** The peptide labeling reagents *N,N*-dimethyl-7-aminocoumarin-4-acetic acid succinimidyl ester (DAMCA-SE) and 1-pyrenebutanoic acid were purchased from Molecular Probes (Eugene, OR). The activating agents HATU and HOAT were purchased from Applied Biosystems, and the detergent [*N,N*-dimethyl-*n*-dodecylamine *N*-oxide (LDAO)] was from Fluka.

**Synthesis, Labeling, and Purification of the HER Transmembrane Domains.** The HER2 peptide was synthesized using standard Fmoc chemistry on a PerSeptive Biosystems Pioneer peptide synthesizer. Other peptides were supplied protected and resin-bound by Neosystem (Strasbourg, France).

For labeling, pyrenebutanoic acid was activated by HATU and HOAT and used at a 10-fold excess on the free N-terminal amino group of the resin-bound and fully protected peptides under basic conditions. The mixture was allowed to react at room temperature with vortexing for 2 h protected from light. Coumarin labeling was performed with DMACA succinimidyl ester at a 10-fold excess in dimethyl sulfoxide on the resin-bound peptide. The reaction was allowed to proceed at room temperature for 6 h in the dark. Resins were washed six times with dimethylformamide and three times with dichloromethane. Peptides were cleaved and side chains deprotected at the same time for 1 h with a cocktail of 80% trifluoroacetic acid (TFA), 10% thioanisole, 5% ethanedithiol, and 5% ultrapure water. Cleaved peptides were precipitated with ice-cold *tert*-butyl methyl ether and centrifuged, and the pellets were washed three times with the same solvent. Peptides were dried, resolubilized in 25  $\mu$ L of 100% TFA, and immediately diluted 40-fold with trifluoroethanol (TFE). The solution was passed through a 0.2  $\mu$ m filter (Millex LG, Millipore) and dried.

For purification, crude peptide powder was dissolved in 10–50  $\mu$ L of TFA, immediately followed by 500  $\mu$ L of TFE. Aliquots of 50–200  $\mu$ L were adjusted to a volume of 1 mL by addition of 60% solvent B (2.8/1 propan-2-ol/acetonitrile mixture with 0.3% TFA) and 40% solvent A (water with 0.3% TFA). The solution was loaded onto a C4 semipreparative HPLC column (Macherey-Nagel, Strasbourg, France) and eluted with a gradient from 60 to 85% B. This protocol allows the separation of labeled and unlabeled peptides to homogeneity (>95%) but at the expense of low yields (often <5%). Mass spectrometry was used to confirm the presence of the purified peptide. The molar extinction coefficients measured for pyrene-labeled ( $\epsilon_{342} = 32\,000$ ) and for coumarin-labeled ( $\epsilon_{373} = 16\,500$ ) peptides were as previously measured for the labeled glycophorin A transmembrane peptides (30).

**Reconstitution in Detergent Micelles.** For reconstitution into detergent solution, an equimolar mixture of pyrene- and coumarin-labeled peptides was adjusted to 50–500  $\mu$ M total peptides in TFE. The required amount of peptide solution (10–100  $\mu$ L) was mixed with a concentrated detergent solution to produce a detergent peptide ratio of 500/1. This solution was dried under vacuum, and the resulting film was

solubilized in 10 mM phosphate buffer (pH 7) and 100 mM NaCl. Reconstituted peptides were adjusted to the desired peptide and detergent concentration in buffer.

**FRET Measurements.** Fluorescence measurements were taken as described previously (15, 30). To convert the observed spectrum to the fraction of dimer ( $\alpha$ ), the ratio of the pyrene-sensitized emission to the direct coumarin emission was normalized using the ratio observed when all the peptides are dimeric (0.75 for homodimers and 1.5 for heterodimers). It was observed, using solutions containing only the pyrene-labeled peptides, that for HER2tm, a very small fraction of dimers gave a pyrene excimer signal. So, in measurements that included those peptides, it was necessary to introduce a small correction.

**Data Analysis.** Models describing the expected FRET as a function of concentration and equilibrium constants were constructed using a spreadsheet in which the free model parameters were adjusted to minimize  $\chi^2$ ; this adjustment was done automatically using the solver integrated in Excel.

The homodimerization model was the same as that used previously (30). If one defines  $C_0$  as the total peptide concentration and  $\alpha$  as the fraction in dimers, the concentration of monomeric peptide ( $[M]$ ) is given by eq 1, the concentration of dimers ( $[D]$ ) by eq 2, and the dissociation constant ( $K_d$ ) by eq 3.

$$[M] = (1 - \alpha)C_0 \quad (1)$$

$$[D] = \alpha \frac{C_0}{2} \quad (2)$$

$$K_d = \frac{[M]^2}{[D]} \quad (3)$$

$$K_d = 2C_0 \frac{(1 - \alpha)^2}{\alpha} \quad (4)$$

Combining eqs 1–3, we obtain eq 4 for the relation between the dissociation constant and the fraction of dimers. The second-order polynomial expansion of eq 4 has a single positive real root, eq 5 which is used to model the experimental data ( $\alpha$ ) by adjusting the single free variable,  $K_d$ .

$$\alpha = \left( \sqrt{1 + \frac{K_d}{8C_0}} - \sqrt{\frac{K_d}{8C_0}} \right)^2 \quad (5)$$

In the heterodimerization model, we consider the three linked dimerization equilibria; homodimerizations of species A and B are defined by two homomeric dissociation constants ( $K_a$  and  $K_b$ , respectively), and the third equilibrium is defined by a heteromeric dissociation constant ( $K_{ab}$ ) (eqs 6–8). Here  $[A]$ ,  $[B]$ ,  $[AA]$ ,  $[BB]$ , and  $[AB]$  are the concentrations of monomers A and B, the two homodimers, and the heterodimeric species, respectively.

$$K_a = \frac{[A]^2}{[AA]} \quad (6)$$

$$K_b = \frac{[B]^2}{[BB]} \quad (7)$$

$$K_{ab} = \frac{[A][B]}{[AB]} \quad (8)$$

The concentrations of all species can be linked to  $[A]$ , the concentration of the first monomer, and  $[AA]$  directly from eq 6 (eq 9)

$$[AA] = \frac{[A]^2}{K_a} \quad (9)$$

By experimental design, the total concentration of the A species is always equal to that of the B species; this facilitates the analysis. Using eqs 10 and 11, which follow from this condition, and combining with eq 7, we obtain a second-order polynomial expansion (eq 12). This equation has a single positive real root, allowing determination of the concentrations of B (eq 13) and BB by substitution in eq 7, in terms of  $[A]$  and the homodimerization equilibrium constants. By substituting in eq 8, we can obtain the concentrations of all the components in terms of  $[A]$  and the three equilibrium constants.

$$[A] + 2[AA] = [B] + 2[BB] \quad (10)$$

$$[BB] = \frac{[A] + 2[AA] - [B]}{2} \quad (11)$$

$$2[B]^2 + K_b[B] - K_b([A] + 2[AA]) = 0 \quad (12)$$

$$[B] = [-K_b + \sqrt{K_b^2 + 8K_b([A] + 2[AA])}] / 4 \quad (13)$$

We can thus describe the normalized heterodimer data ( $\alpha$ ) (eq 14) in terms of  $[A]$  and the different equilibrium constants.

$$\alpha = \frac{[AB]}{([A] + 2[AA] + [AB])} = \frac{-K_b + \sqrt{K_b^2 + 8K_b\left([A] + 2\frac{[A]^2}{K_a}\right)}}{4K_{ab}\left(1 + \frac{[A]}{K_a}\right) + \left[-K_b + \sqrt{K_b^2 + 8K_b\left([A] + 2\frac{[A]^2}{K_a}\right)}\right]} \quad (14)$$

To adjust this numerical model to fit the experimental data, we proceeded as follows. First, the homodimerization constants  $K_a$  and  $K_b$ , determined above, were inserted into the model. Then two subsequent steps were repeated until convergence. The values of  $[A]$  are adjusted so that the calculated total concentration of A matched those of the experiment. Then the solver macro of Excel is used to obtain the optimal value of  $K_{ab}$  by minimizing the  $\chi^2$  between experimental and modeled data.

**CD Measurement.** Samples were prepared as mentioned previously using more concentrated but less purified material (60–70% purity) to reach 10  $\mu$ M peptides in 10 mM LDAO. Concentrations were adjusted on the basis of the fluorochrome absorbance. Circular dichroism spectra were recorded on a Jasco 810 dichrograph using 1 mm thick quartz cells in 10 mM sodium phosphate (pH 7) at 20 °C. CD spectra were measured between 190 and 260 nm at 0.2 nm/min and

were averaged from three independent acquisitions. Mean ellipticity values per residue ( $[\Theta]$ ) were calculated with the relation  $[\Theta] = 3300m\Delta A/(lcn)$ , where  $l$  (path length) is 0.1 cm,  $n$  the number of residues,  $m$  the molecular mass in daltons, and  $c$  the protein concentration expressed in milligrams per milliliter. The numbers of residues ( $n$ ) were 32 for HER1, HER3, and HER4 and 33 for HER2, whereas molecular masses were 3333.2, 3348.1, 3604.4, and 3301.1 Da for HER1–4, respectively.

**Building the EGFR Transmembrane Domain on the Crystal Structure of the Dimeric Extracellular Domain.** The Deep view program (31) was used to build the various structural models presented here. The models were based on the known structures of EGFR (PDB entry 1IVO), HER3 (PDB entry 1M6B), and glycophorin A (PDB entry 1AFO).

The procedure that was used comprised four steps: (i) the reconstruction of domain IV of EGFR by the threading of the sequence of the second cysteine rich region of EGFR onto the equivalent region of the HER3 structure (this was straightforward because of the conservation of the cysteine residues and their importance for the structure), (ii) superposition of this model structure on each equivalent partial structure included in the dimeric EGFR structure, (iii) ligation of the modeled structures at the C-terminus of the experimental ones, and (iv) minimization of the internal energy of the resulting model structure using 100 steps of steepest descent, in a vacuum excluding electrostatic interactions.

To illustrate how the transmembrane region might extend the dimer interface, we further expanded the model by two additional juxtamembrane loops (four and six residues long depending on the monomer) followed by a dimeric transmembrane domain modeled on the structure of the glycophorin A dimer. This transmembrane domain model was made by aligning the first SmXXXSm motif of the EGFR transmembrane domain (Gly<sub>625</sub>XXXAla<sub>629</sub>) with the GlyXXXGly motif of glycophorin A, and the energy of the dimeric structure that includes the transmembrane domain and juxtamembrane residues was minimized to remove clashes. This procedure did not modify the main features of the dimer. Then the dimeric EGFR transmembrane region was manually placed under the EGFR dimeric interface, extending the pseudo- $C_2$  axis, and the backbones were ligated and the loops optimized. It should be noted that the alternate EGFR extracellular structures (PDB entry 1MOX) were also used as input for the modeling. Among the differences, the later is 11 residues shorter and the two monomers are asymmetric, especially at the level of the orientation of the C-terminal extremities. In this case, the model gives rise to the same global features concerning the induced proximities between the transmembrane domains, but the asymmetry is maintained which is interesting but beyond the scope of this work.

## RESULTS

**Quantitative Assessment of Transmembrane Domain Interactions.** To assess interactions between the transmembrane helices, we have used the fluorescence assay developed by Fisher et al. (30). In this assay, fluorescently labeled synthetic peptides interact in detergent solution and the interaction is measured as the level of resonance energy transfer (FRET) between a donor and an acceptor fluorophore. By using pyrene as the donor fluorophore and coumarin as the

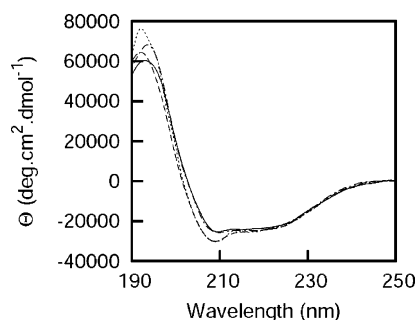


FIGURE 2: Circular dichroism spectra of the four HER transmembrane domains (10  $\mu$ M peptide in 10 mM LDAO): EGFRtm (—), HER2tm (---), HER3tm (- · -), and HER4tm (- - -).

acceptor, the characteristic transfer distance is relatively long and thus the FRET signal is independent of the details of complex geometry. FRET is measured from excitation spectra which allow the robust and simultaneous estimation of pyrene-sensitized emission and coumarin concentration.

Experiments have been set up in LDAO detergent that, on the basis of our previous experience with GpA and HER2 homodimers, has been proven to be ideal. First, because LDAO is not too dissociating as a detergent (in contrast with, for example, SDS), it makes measurement of weakly interacting peptides possible without too much nonspecific association. Second, thermodynamic equilibrium is reached relatively quickly (in contrast with, for example, DPC), making measurements easier and less fastidious. Third, it is chemically and biologically stable and available at high purity, in contrast with many detergents (for example, glycosylated alcohols, or zwittergents) where hydrolysis, anomeric mixtures, and UV-absorbing impurities are often a problem.

We synthesized peptides corresponding to the transmembrane sequences (tm) of EGFR, HER2, HER3, and HER4 (Figure 1). Several minor modifications were made to the sequences to facilitate our measurements as described in Materials and Methods. Each of these peptides was then labeled on the N-terminus with either pyrene or coumarin. To ensure that measured dissociation constants correspond to the association of similarly structured peptides, we verified the secondary structure of the different peptides by CD spectroscopy at the same micellar detergent to peptide ratio used for fluorescence studies (10  $\mu$ M peptides in 10 mM LDAO). Figure 2 shows CD traces characteristic of mainly  $\alpha$ -helical peptides, with HER1 being identical to HER4 and HER2 more closely related to HER3. It is important to note here that HER1 and HER4 have a very different behavior in term of interaction (vide infra).

Figure 3A shows the evolution of the excitation spectrum during a titration of a peptide solution that contains an equimolar mixture of peptide labeled with coumarin and pyrene. The coumarin excitation peak at 374 nm gives an estimation of the total peptide concentration, while the narrow pyrene-sensitized excitation peak at 343 nm provides an estimation of the concentration of dimers containing a pyrene-labeled peptide and a coumarin-labeled peptide. As each spectrum gives information about dimer concentration and total concentration, for a fixed mixture, this method gives a robust estimation of the fraction of peptides in dimers. Examination of the sensitivity of dimer formation to the detergent concentration in the range of 1 mM [just under

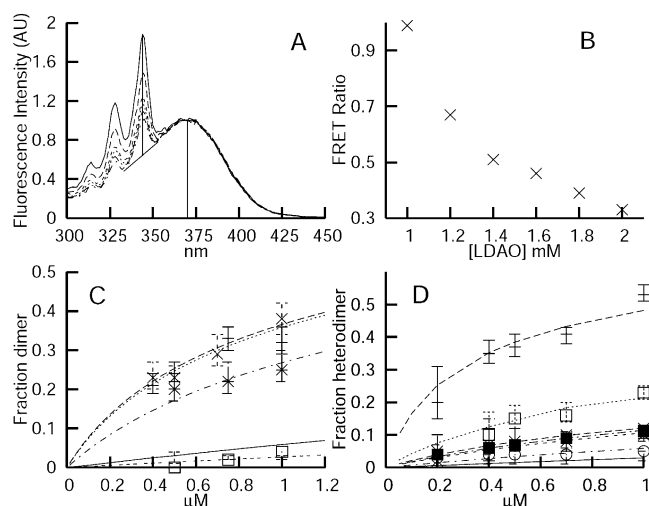


FIGURE 3: Measurements of the level of transmembrane helix dimerization. (A) Excitation spectra of solutions containing equimolar concentrations of coumarin-labeled HER2tm and pyrene-labeled HER2tm (1  $\mu$ M total peptide). Emission was measured at 500 nm where only fluorescence from the coumarin chromophore is observed. The maximum at 370 nm (···) is proportional to the total amount of peptides. The sharp signal observed at 343 nm (—) is characteristic of the pyrene excitation. This sensitized contribution to the coumarin emission occurs only when complexes are formed between the two labeled peptides. The signal above the oblique dashed line is proportional to the concentration of the dimeric species. The ratio of the sensitized emission (measured at 343 nm) to the intensity of direct fluorescence (measured at 370 nm) (FRET ratio) is proportional to the fraction of the dimeric species. This signal changes upon addition of detergent or dilution. Shown are a series of spectra with detergent concentrations between 1 (top) and 2 mM (bottom). (B) Corresponding evolution of the FRET ratio as a function of LDAO concentration. (C) Evolution of the fraction of dimers with peptide concentration for homodimer formation. HER2tm ( $\times$ ), EGFRtm (+), HER3tm (\*), and HER4tm ( $\square$ ) with the fitted lines corresponding to  $K_{dapp}$  values of 2.2, 2.3, 4, and 70  $\mu$ M, respectively. In each case, spectra were measured in the presence of 2 mM LDAO. The solid line indicates the expected occurrence of nonspecific dimers following the simple distribution of peptides among available micelles. (D) Evolution of the fraction of heterodimers with concentration. For each of the six possible heterodimers, the observed (points) and fitted (lines) fractions of dimers are shown. From top to bottom: EGFRtm–HER2tm (+), HER2tm–HER3tm ( $\square$ ), HER2tm–HER4tm ( $\times$ ), EGFR–HER3tms (\*), EGFR–HER4tms ( $\blacksquare$ ), and HER4tm–HER3tm ( $\circ$ ). The solid line represents the highest possible level of nonspecific heterodimers assuming that none of the peptides can specifically self-associate.

the critical micellar concentration (cmc) of the detergent] to 2 mM is shown in Figure 3B. As expected (15), below the cmc we observe a rapid increase in the apparent fraction of dimers due to the formation of higher-order aggregates, above the cmc a more usual sensitivity. It was previously shown that the apparent free energy of interaction is in first approximation related to the logarithm of micellar detergent concentration (15). In the case presented here, the gradient of the sensitivity appears to be  $\sim 7$  kJ/mol. At a detergent concentration of 2 mM, the FRET signal remains sufficiently high to allow the analysis of the dissociation constant following peptide dilution. Also, there is sufficient detergent that small concentration errors do not impair the precision of the measurement. Finally, it is important to note that the micellar concentration of the detergent is 1000-fold higher than the maximum peptide concentration that was used. Given the cmc of LDAO (1.1 mM) and its aggregation number ( $N = 76$ ) (15), there is an excess of free micelles in

Table 1: Hierarchy of Dimerization Affinities<sup>a</sup>

dimeric species	$K_{dapp}$ ( $\mu$ M)	$\Delta G^\circ$ (kJ/mol)	$\Delta\Delta G^\circ$ (kJ/mol)
EGFRtm–2tm	$0.20 \pm 0.05$	38.3	0
HER2tm–3tm	$0.85 \pm 0.25$	34.6	3.6
EGFRtm–3tm	$2.0 \pm 0.9$	32.4	5.9
HER2tm–2tm	$2.2 \pm 0.5$	32.3	6
EGFRtm–EGFRtm	$2.3 \pm 0.8$	32.1	6.1
HER2tm–4tm	$2.6 \pm 0.5$	31.9	6.4
EGFRtm–4tm	$2.9 \pm 0.7$	31.6	6.6
HER3tm–3tm	$4.0 \pm 0.5$	30.8	7.5
HER3tm–4tm	$6.2 \pm 1.6$	29.7	8.6
HER4tm–4tm	$70 \pm 20$	23.7	14.6

<sup>a</sup> The dissociation constants obtained for the different dimeric species ( $K_{dapp}$ ) together with the calculated standard free energy of dissociation ( $\Delta G^\circ$ ) and, in the last column, the difference between the standard free energy of dissociation and that of the most strongly dimerizing pair, EGFRtm–HER2tm ( $\Delta\Delta G^\circ$ ).  $K_{dapp}$  is the best fit (very similar to the mean)  $\pm$  the standard error.

2 mM LDAO. Consequently, the FRET signal from unasociated peptides within the same micelle by chance is weak. However, this so-called stochastic distribution of peptides among micelles does not give zero dimer population, and to illustrate its contribution, it was roughly modeled as a Poisson distribution using the peptide/micelle ratio as the mean probability of finding a peptide within a micelle. This detergent concentration was chosen for the remaining experiments.

**Self-Association of HER Transmembrane Domains.** Figure 3C shows the titrations obtained for the different homodimers. In each case, the fraction of dimers was estimated at a series of different total peptide concentrations. The indicated error bars not only take into account the standard deviation from repeated measurements but also include an error based on the propagation of all uncertainties involved in the measurement. The lines show the best fit to the data obtained using the model developed previously by adjusting the dissociation constant (15, 30). The dissociation constants determined are listed in Table 1. The fitting gives relatively robust estimates of the various dissociation constants, with the notable exception of that of the HER4tm homodimer. This peptide appears almost unable to homodimerize, and thus, the observed FRET corresponds to the level anticipated from the nonspecific distribution of peptides among available micelles. Nevertheless, the very small signal assigned to FRET for the highest peptide concentrations allows an estimation of this nonspecific dissociation constant. It is clear that using this in vitro assay we were able to measure values of dissociation constants for the transmembrane domains of each of the four members of the HER receptor family. These peptides show a wide range of dimerization abilities with dissociation constants ranging from  $\sim 2$   $\mu$ M for EGFRtm and HER2tm to nearly 100  $\mu$ M for HER4tm. It was found that HER3tm does not self-associate as easily as EGFRtm and HER2tm but had a  $K_d$  on the same order of magnitude, near 4  $\mu$ M. For comparison, the glycoprotein A tm was previously found to have a  $K_d$  1 order of magnitude lower under similar conditions (15, 30). Building on these results, we turned our attention to the ability of these different peptides to form heterodimers.

To treat heterodimer formation, one cannot directly use the simple model developed for homodimers. Although the FRET signal comes only from the heterodimers present in

the mixture, the two homodimeric species are also present and participate in linked equilibria. These linked reactions modify the availability of monomers differently for the two transmembrane domains. Finding an analytical solution to describe the heterodimer concentration as a function of total concentrations in the presence of three linked equilibria is not trivial. So we preferred to develop a numerical model (see Materials and Methods) in which the concentrations of the various species present in the solution are calculated from the concentrations of one monomeric species given the three different dimer dissociation constants (two homodimers and one heterodimer) and the known stoichiometry of the mixture. In this model, the one free variable used for fitting is the heterodimeric dissociation constant, the homodimeric dissociation constants having been already determined (see above) and the total concentrations of the labeled peptides being known.

**Heterodimers and a Hierarchy of Affinities.** Figure 3D shows the evolution of the heterodimeric fraction as a function of the total peptide concentrations for the six possible heterologous mixtures. Again the error bars are estimations of the precision of the different points, and the lines show the best fit to the data obtained by modifying the heterodimer dissociation constant. These dissociation constants are collected in Table 1. It is immediately apparent that the ability of the different transmembrane helix pairs to form dimers varies greatly; thus, the EGFRtm–HER2tm pair gives a strong FRET signal over a wide range of concentrations, while other pairs give weaker signals. To test the robustness of the model, we measured the sensitivity of our heterodimer dissociation constants to errors in homodimer dissociation constants. It was found that changing the homodimer  $K_d$  values by their estimated errors did not alter the heterodimeric  $K_d$  by more than 5%, indicating that the estimates are robust.

The EGFRtm–HER2tm pair gave a particularly high affinity ( $K_d = 200$  nM), 10 times higher than the EGFRtm and HER2tm homodimer affinities. These two transmembrane helices are thus able to self-associate but prefer to form a heterodimer. Besides this particularly high-affinity, HER2tm–HER3tm heterodimer also displayed a very high affinity ( $K_d = 800$  nM). Three of the remaining heterodimers form with a dissociation constant similar to those of the EGFRtm and HER2tm homodimers. Finally, the association of HER3tm and HER4tm gives a higher dissociation constant ( $K_d = 6.2$   $\mu$ M). The solid line in Figure 3D representing the nonspecific heterodimeric association is an upper range limit that considers that none of the three possible dimers are able to form specifically. To summarize these results, the hierarchy of HERtm peptide dimerization is shown in Table 1. The apparent dissociation constant ( $K_d$ ) in 2 mM LDAO for each pair is shown together with the calculated standard free energy change of dissociation ( $\Delta G^\circ$ ) and the difference between this last value and that observed for the highest-affinity EGFRtm–HER2tm heterodimer ( $\Delta\Delta G^\circ$ ).

It is difficult to relate the dissociation constants measured in detergent solution to the behavior in the plasma membrane, or in the different domains of the membrane. However, in line with the literature on GpA dimerization (16, 32–35), while the absolute dissociation constants and free energy changes are very sensitive to the amphiphile environment (15), we expect the free energy differences to be less

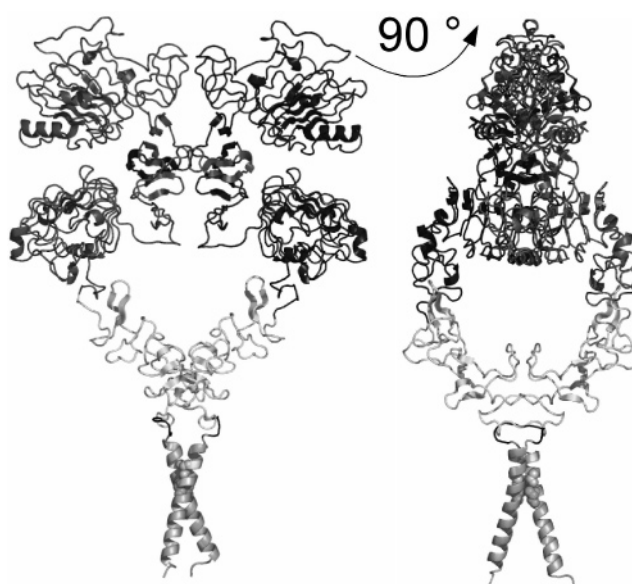


FIGURE 4: Reconstructed models of dimeric EGFR. In the dimeric EGFR model, colored dark gray are the two soluble domains in the crystal structure and colored light gray is the cysteine rich domain. The short (four-residue) juxtamembrane loop is colored black. The dimeric transmembrane domain was arbitrarily modeled on the structures of the glycophorin A tm using as a template the first SmXXXSm motif of EGFRtm.

sensitive, as long as there are no specific interactions (16, 35). Thus, in the cell membrane, we expect the 6 kJ/mol difference between the free energy changes of dissociation of the EGFR–HER2 and HER2–HER2 pairs to be approximately preserved and thus the 11-fold difference in dissociation constants to persist in different environments.

**Structural Evidence for Transmembrane Domain Interaction in Receptor Dimers.** To appreciate the possible role of the transmembrane helices in the context of the intact receptor, it is useful to have a structural model of the membrane-associated receptors in the dimeric open configuration to determine if transmembrane helix association is possible in the dimeric form and if the dissociation constants we have measured could be important in the context of the intact receptor. The model that we have constructed is shown in Figure 4. Briefly, this model was constructed from the dimeric crystal structure of the EGFR ECD [PDB entry 1IVO (36)] by addition of the missing cysteine rich region extracted from the crystal structure of the HER3 ECD [PDB entry 1M6B (37)]. This extension was particularly easy as the EGFR structure contains part of this well-conserved and structurally rigid region allowing easy alignment of the two structures. This extension did not generate any clashes, and remarkably, the protruding loop of this cysteine rich region is in a position to make an additional intermolecular contact. This area is involved in an intramolecular interaction in the presumably autoinhibited “tethered” configuration (37, 38). Most importantly, the C-terminal extremities of these cysteine rich regions fall only 12 Å apart. This distance is ideally suited for extension of the model with a dimer of helical transmembrane domains, which we have modeled arbitrarily on the dimeric glycophorin A transmembrane structure [PDB entry 1AFO (39)]. A similar feature was depicted in a dimeric model of a nearly full length HER-2 receptor (40). For the purpose of representation, the four-residue peptide that makes the junction between the ECD and the transmembrane helix

is colored black. It is important to remark that though the transmembrane helical dimer based on glycoporphin A is compatible with the modeled ECDs there is sufficient flexibility that many different dimeric transmembrane structures are equally compatible.

This model shows a number of important features. First, the dimeric structure of the ECD not only is compatible with a dimeric transmembrane domain but also would seem almost to require it. It is thus probable that dimerization of the transmembrane and ECDs are linked, each contributing to the overall receptor dissociation constant. Second, the model would suggest that beyond the protruding loop in the first cysteine rich domain that constitutes the dimerization arm, the equivalent loop in the second cysteine rich domain and the transmembrane helices participate in the interface.

## DISCUSSION

We have shown that transmembrane domains of the four HER receptors are able to homo- and heterodimerize in vitro with a 3 order of magnitude range in the apparent  $K_d$  values. This complex hierarchy of interaction specificity was observed despite the reduced level of sequence complexity observed in transmembrane sequences. Furthermore, the structure of the ECD of the EGFR dimer suggests a role for transmembrane domain dimerization in the activation process. However, it is important to establish how the dimerization energetics demonstrated here compare with those of other measured interactions in similar or distinct environments. Then we will address the question of the role transmembrane helix association could play in the overall monomer–dimer equilibrium and how this could influence the function of these particular bitopic receptors.

The lowest dissociation constants that we have determined for the HERtm dimers are 1 order of magnitude weaker than that measured for glycoporphin A, the best characterized specific transmembrane domain interaction, using the same FRET method and environment (30). This lower affinity is perhaps what is to be expected for a dynamic and functionally important association, as opposed to the more static and structural association of the glycoporphin A transmembrane helix. The reduced affinity and the high sensitivity of the dimers to the detergent concentration could explain the difficulties encountered by Stanley and Fleming (17) in precisely characterizing the thermodynamics of HERtm associations using sedimentation equilibrium analytical ultracentrifugation. This technique requires larger amounts of a fusion protein at a higher detergent concentration; it also results in higher protein to detergent ratios and consequent problems due to nonspecific association. In agreement with Stanley and Fleming, we find that the dimerization of HERtm's is not strong in detergent micelles. We are, however, able to measure the different dissociation constants which are largely, though not entirely, in agreement with the observations made using a genetic assay (TOXCAT), where the ability of the HER transmembrane domains to self-associate in the inner membrane of *Escherichia coli* was determined (26). The major difference between our results and those of Mendrola et al. concerns HER4tm homodimerization which we find to be particularly weak, while they find it to be by far the strongest.

Tanner and Kyte (41) observed that a recombinant fragment of EGFR, including both the extracellular and

transmembrane domains, had a 10000-fold lower  $K_d$  for dimerization than the soluble ECD. It is difficult to directly compare their results with ours; however, on the basis of our measurement of the EGFRtm free energy of dimerization, the range of detergent sensitivities observed for HER2tm and glycoporphin A transmembrane domains (ref 15 and unpublished results), we can estimate a contribution of the EGFR transmembrane helix in 1% Triton X-100 to dimer dissociation of 19.9–23.5 kJ/mol. This compares very favorably with the 10000-fold stabilization (e.g., 20.9 kJ/mol) reported by Tanner, possibly indicating that the dimerization ability of EGFRtm is approximately the same in the context of the isolated transmembrane domain and the linked transmembrane and ECDs with bound EGF. It has been argued that the poor homodimerization of the EGFR ECD in Tanner and Kyte's studies originates from the details of their purification protocol (42). Some variability of this type is not surprising in view of the detailed changes that regulate the receptor association following ligand binding. Nevertheless, the size of the effect of adding the transmembrane helix (20 kJ/mol) is much greater than that attributed to protocol differences (6 kJ/mol).

The dimeric crystal structure of the liganded EGFR provides a picture of the interactions that occur upon ligand binding (36, 43). Also, the description of a dimerization arm within the dimer interface reinforces the idea that the ECD is the major contributor to the association process and receptor activation (44). However, the observation of Tanner and co-workers favors a possible contribution of the single transmembrane domain to the overall association energetics. Other studies also show that in most cases the ECD does not encode all the interactions needed for whole receptor oligomerization.

Using multiangle laser light scattering and sedimentation equilibrium analytical ultracentrifugation in a study of isolated ECDs, Ferguson and co-workers (42) proposed that ligands induce efficient homodimerization of the EGFR and HER4 ECDs at least in the submicromolar range. However, in contrast, ligands were unable to drive self-association of the HER3 ECD and five of the six potential heterodimers. Also, the orphan HER2 ECD was not observed to dimerize. The authors suggested that regions outside this domain were required for the corresponding dimeric interactions. Because of the fact that the dimeric structures of the ECDs favor direct interaction between transmembrane domains, we propose that the receptor transmembrane domains are one of the contributors to the association of intact receptors.

In the case of the HER2 receptor, genetic alterations that displace the equilibrium toward the aggregated forms (including overexpression or mutations within the tm) also suggest that other domains are involved in the tendency of HER2 to self-aggregate. The energetics of transmembrane helix dimerization that we observe can drive the formation of HER2 dimers if the receptor cell surface concentration becomes sufficiently high.

Further, HER2tm has an even greater tendency to heterodimerize with HER3tm and EGFRtm, in agreement with in vivo measurements and in contrast to what happens with the isolated ECD (42). In such cases, the contribution of transmembrane helix dimerization to signal transduction could appear to be even more important.

An intriguing line of evidence in favor of a role for the transmembrane domains in modulating whole receptor dimerization is the observed correlation of preferred partners we have determined for transmembrane domains here with that previously determined for intact receptors (19, 21, 45, 46). As for our study, HER2 is considered to be the preferential partner for the other receptors, with a marked preference for HER3 and EGFR. Similarly, the HER4 heterodimer with HER2 appears to be less favored. The other types of heterodimers that involve EGFR were also observed but were more easily detectable in the absence of HER2; these observations are also eased by EGFR overexpression. Finally, the existence of the heterodimeric HER3–HER4 species was never documented to our knowledge and was not detected in experiments by Tzahar et al., who detected eight of the ten potential dimeric arrangements of the receptors. It is the least favored heterodimer in our experiments. However, it should be noted that although the HER4 tm was not found to homodimerize in our experiment, the cellular signaling by HER4 has been frequently documented, particularly in the development of the nervous system (47, 48). This illustrates that our simplified assay cannot evidently account for the entire complexity of the whole receptor in the cellular context. In that case, other domains or a modulation by the environment would dominate the dimerization process. However, the correlation between the *in vivo* and *in vitro* studies strengthens the idea of a contribution for the transmembrane domains in the association, and particularly in influencing specificity and selectivity. Such correlation suggests that the transmembrane domains encode much of the intrinsic homodimerization versus heterodimerization preferences of the whole receptors. In the normal cell, this implies that after the relative expression level of each receptor and the availability of their cognate ligands, the transmembrane domain will be a selector of the population of dimeric species that will be activated. Of course, this should be confirmed in a cellular context; nevertheless, we illustrate the effect of the measured interaction hierarchy in Figure 5, for a system with three different receptor types: EGFR, HER2, and HER3. According to the relative levels of different receptors, the population of dimeric species on the cell surface will change. In Figure 5, we consider a system with a constant total number of active receptors and delineate the areas where various types of heterodimers are particularly common. Thus, for many different compositions, the EGFR–HER2 dimer is the most abundant, while the EGFR–HER3 dimer is only abundant for very specific compositions, due to the higher EGFR–EGFR, EGFR–HER2, and HER2–HER3 affinities. Clearly, the diagram is unable to represent the full complexity of the interplay of the different receptors where (i) four receptors can associate depending on the conformation of their ECDs, (ii) different conformations are modified as a result of their diverse ligand preferences and (iii) depending on the affinities of the transmembrane domains, and (iv) this in a cellular context with a continuous flow of receptors to and from the cell surface. This diagram does, however, clarify why the HER2 homodimer can be significantly populated only when it is expressed alone at the cell surface (49). As the preferred partner for the other receptors, this homodimer is only common member for a restricted set of compositions. Among the six possible heterodimers, the EGFR–HER2 and HER2–

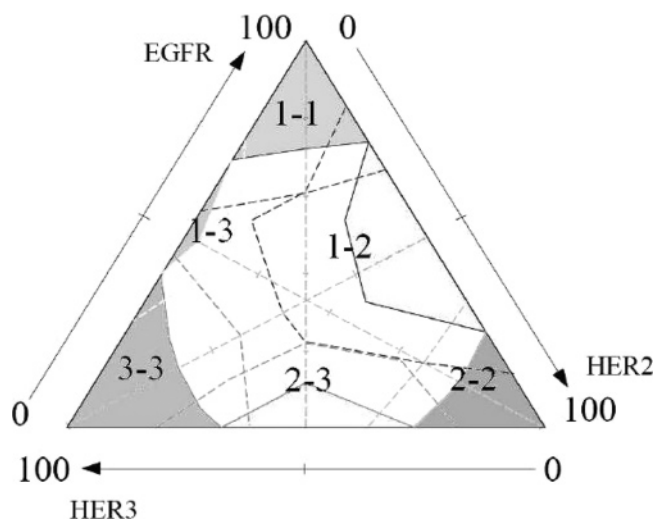


FIGURE 5: Map showing how the measured  $\Delta\Delta G$  differences bias dimer populations. The map shows the major dimeric species that exist for different compositions of dimerizable receptors as calculated from our measurements (Table 1). For the sake of simplicity, the situation that is shown corresponds to a constant, and high, total amount of receptors. Pure populations are found at the corners of the triangle, two component mixtures along the edges and three component mixtures within the triangle. Gray shading surrounds areas where more than 50% of the receptors are found as a single type of dimer, and dashed lines surround areas corresponding to 33%. The different gray tones are used for different dimers. For the sake of simplicity, the value for EGFR is 1.

HER3 pairs are the most documented in the literature, which, given the thermodynamics defined in this study and illustrated in Figure 5, are common over a large range of compositions.

Cancer cells frequently express multiple HER receptors. The complexity of the mixture behavior affirmed from this study may explain the difficulty and the contradictory results that come from clinical studies with the aim of investigating the correlations between HER expression and prognosis factor for tumor evolution (50).

## CONCLUSION

Using synthetic hydrophobic peptides corresponding to the transmembrane domains of the HER receptors, we have been able to decipher the cross affinity of these domains in homo- and heterodimeric contexts. One success of the approach is the fact that we are able to quantify relatively weak interactions that could be missed by using other less sensitive methods. A variety of apparent dissociation constants ranging from 0.1 to 100  $\mu\text{M}$  were observed, showing that transmembrane domains, even if greatly enriched in hydrophobic residues, and thus with a reduced level of sequence complexity, can govern a complex hierarchy of interactions. Using the molecular structure of the dimeric ECDs of EGFR as templates, we show how the transmembrane domain can prolong the dimer interface between the receptors. Furthermore, this structure rationalizes our finding that the hierarchy of transmembrane domain interactions within an artificial environment follows that of the full receptors in a cellular context. We propose that the energetics of transmembrane domain interactions of the HER receptor family play a major role in modulating the affinity, specificity, and selection of partners by receptors during signal transduction. Future work should address the impact of such an interaction hierarchy

at the level of the whole receptors embedded in the membrane of the living cell.

## ACKNOWLEDGMENT

We thank Pierre Hubert for many discussions and his careful reading of the manuscript and useful suggestions.

## REFERENCES

- Mackenzie, K. R. (2006) Folding and stability of  $\alpha$ -helical integral membrane proteins, *Chem. Rev.* 106, 1931–1977.
- Popot, J. L., and Engelman, D. M. (2000) Helical membrane protein folding, stability, and evolution, *Annu. Rev. Biochem.* 69, 881–922.
- Prodohl, A., Volkmer, T., Finger, C., and Schneider, D. (2005) Defining the structural basis for assembly of a transmembrane cytochrome, *J. Mol. Biol.* 350, 744–756.
- Ulmschneider, M. B., Tieleman, D. P., and Sansom, M. S. P. (2005) The role of extra-membranous inter-helical loops in helix-helix interactions, *Protein Eng., Des. Sel.* 18, 563–570.
- Granseth, E., von Heijne, G., and Elofsson, A. (2005) A study of the membrane-water interface region of membrane proteins, *J. Mol. Biol.* 346, 377–385.
- Orgel, J. P. R. O. (2004) Sequence context and modified hydrophobic moment plots help identify ‘horizontal’ surface helices in transmembrane protein structure prediction, *J. Struct. Biol.* 148, 51–65.
- Arkin, I. T. (2002) Structural aspects of oligomerization taking place between the transmembrane  $\alpha$ -helices of bitopic membrane proteins, *Biochim. Biophys. Acta* 1565, 347–363.
- Brosig, B., and Langosch, D. (1998) The dimerization motif of the glycophorin A transmembrane segment in membranes: Importance of glycine residues, *Protein Sci.* 7, 1052–1056.
- Russ, W. P., and Engelman, D. M. (2000) The GxxxG motif: A framework for transmembrane helix-helix association, *J. Mol. Biol.* 296, 911–919.
- Schneider, D., Liu, Y., Gerstein, M., and Engelman, D. M. (2002) Thermostability of membrane protein helix-helix interaction elucidated by statistical analysis, *FEBS Lett.* 532, 231–236.
- Senes, A., Gerstein, M., and Engelman, D. M. (2000) Statistical analysis of amino acid patterns in transmembrane helices: The GxxxG motif occurs frequently and in association with  $\beta$ -branched residues at neighboring positions, *J. Mol. Biol.* 296, 921–936.
- Eilers, M., Patel, A. B., Liu, W., and Smith, S. O. (2002) Comparison of helix interactions in membrane and soluble  $\alpha$ -bundle proteins, *Biophys. J.* 82, 2720–2736.
- Kleiger, G., Grothe, R., Mallick, P., and Eisenberg, D. (2002) GXXXG and AXXXA: Common  $\alpha$ -helical interaction motifs in proteins, particularly in extremophiles, *Biochemistry* 41, 5990–5997.
- Dawson, J. P., Weinger, J. S., and Engelman, D. M. (2002) Motifs of serine and threonine can drive association of transmembrane helices, *J. Mol. Biol.* 316, 799–805.
- Fisher, L. E., Engelman, D. M., and Sturgis, J. N. (2003) Effect of detergents on the association of the glycophorin A transmembrane helix, *Biophys. J.* 85, 3097–3105.
- Fleming, K. G., and Engelman, D. M. (2001) Specificity in transmembrane helix-helix interactions can define a hierarchy of stability for sequence variants, *Proc. Natl. Acad. Sci. U.S.A.* 98, 14340–14344.
- Stanley, A. M., and Fleming, K. G. (2005) The transmembrane domains of ErbB receptors do not dimerize strongly in micelles, *J. Mol. Biol.* 347, 759–772.
- Merzlyakov, M., You, M., Li, E., and Hristova, K. (2006) Transmembrane helix heterodimerization in lipid bilayers: Probing the energetics behind autosomal dominant growth disorders, *J. Mol. Biol.* 358, 1–7.
- Hynes, N. E., and Lane, H. A. (2005) ERBB receptors and cancer: The complexity of targeted inhibitors, *Nat. Rev. Cancer* 5, 341–354.
- Graus-Porta, D., Beerli, R. R., Daly, J. M., and Hynes, N. E. (1997) ErbB-2, the preferred heterodimerization partner of all ErbB receptors, is a mediator of lateral signaling, *EMBO J.* 16, 1647–1655.
- Tzahar, E., Waterman, H., Chen, X., Levkowitz, G., Karunakaran, D., Lavi, S., Ratzkin, B. J., and Yarden, Y. (1996) A hierarchical network of interreceptor interactions determines signal transduction by Neu differentiation factor/neuregulin and epidermal growth factor, *Mol. Cell. Biol.* 16, 5276–5287.
- Bargmann, C. I., Hung, M. C., and Weinberg, R. A. (1986) Multiple independent activations of the neu oncogene by a point mutation altering the transmembrane domain of p185, *Cell* 45, 649–657.
- Weiner, D. B., Liu, J., Cohen, J. A., Williams, W. V., and Greene, M. I. (1989) A point mutation in the neu oncogene mimics ligand induction of receptor aggregation, *Nature* 339, 230–231.
- Gerber, D., Sal-Man, N., and Shai, Y. (2004) Two motifs within a transmembrane domain, one for homodimerization and the other for heterodimerization, *J. Biol. Chem.* 279, 21177–21182.
- Sternberg, M. J., and Gullick, W. J. (1989) Neu receptor dimerization, *Nature* 339, 587.
- Mendrola, J. M., Berger, M. B., King, M. C., and Lemmon, M. A. (2002) The single transmembrane domains of ErbB receptors self-associate in cell membranes, *J. Biol. Chem.* 277, 4704–4712.
- Lofts, F. J., Hurst, H. C., Sternberg, M. J., and Gullick, W. J. (1993) Specific short transmembrane sequences can inhibit transformation by the mutant neu growth factor receptor in vitro and in vivo, *Oncogene* 8, 2813–2820.
- Bennasroune, A., Fickova, M., Gardin, A., Dirrig-Grosch, S., Aunis, D., Cremel, G., and Hubert, P. (2004) Transmembrane peptides as inhibitors of ErbB receptor signaling, *Mol. Biol. Cell* 15, 3464–3474.
- Bennasroune, A., Gardin, A., Auzan, C., Clauser, E., Dirrig-Grosch, S., Meira, M., Appert-Collin, A., Aunis, D., Cremel, G., and Hubert, P. (2005) Inhibition by transmembrane peptides of chimeric insulin receptors, *Cell. Mol. Life Sci.* 62, 2124–2131.
- Fisher, L. E., Engelman, D. M., and Sturgis, J. N. (1999) Detergents modulate dimerization, but not helicity, of the glycophorin A transmembrane domain, *J. Mol. Biol.* 293, 639–651.
- Guex, N., and Peitsch, M. C. (1997) SWISS-MODEL and the Swiss-PdbViewer: An environment for comparative protein modeling, *Electrophoresis* 18, 2714–2723.
- Lemmon, M. A., Flanagan, J. M., Treutlein, H. R., Zhang, J., and Engelman, D. M. (1992) Sequence specificity in the dimerization of transmembrane  $\alpha$ -helices, *Biochemistry* 31, 12719–12725.
- Lemmon, M. A., Flanagan, J. M., Hunt, J. F., Adair, B. D., Bormann, B. J., Dempsey, C. E., and Engelman, D. M. (1992) Glycophorin A dimerization is driven by specific interactions between transmembrane  $\alpha$ -helices, *J. Biol. Chem.* 267, 7683–7689.
- Brosig, B., and Langosch, D. (1998) The dimerization motif of the glycophorin A transmembrane segment in membranes: Importance of glycine residues, *Protein Sci.* 7, 1052–1056.
- Finger, C., Volkmer, T., Prodohl, A., Otzen, D. E., Engelman, D. M., and Schneider, D. (2006) The stability of transmembrane helix interactions measured in a biological membrane, *J. Mol. Biol.* 358, 1221–1228.
- Ogiso, H., Ishitani, R., Nureki, O., Fukai, S., Yamanaka, M., Kim, J., Saito, K., Sakamoto, A., Inoue, M., Shirouzu, M., and Yokoyama, S. (2002) Crystal structure of the complex of human epidermal growth factor and receptor extracellular domains, *Cell* 110, 775–787.
- Cho, H., and Leahy, D. J. (2002) Structure of the extracellular region of HER3 reveals an interdomain tether, *Science* 297, 1330–1333.
- Ferguson, K. M., Berger, M. B., Mendrola, J. M., Cho, H. S., Leahy, D. J., and Lemmon, M. A. (2003) EGF activates its receptor by removing interactions that autoinhibit ectodomain dimerization, *Mol. Cell* 11, 507–517.
- MacKenzie, K. R., Prestegard, J. H., and Engelman, D. M. (1997) A transmembrane helix dimer: Structure and implications, *Science* 276, 131–133.
- Bagossi, P., Horvath, G., Vereb, G., Szollosi, J., and Tozser, J. (2005) Molecular modeling of nearly full-length ErbB2 receptor, *Biophys. J.* 88, 1354–1363.
- Tanner, K. G., and Kyte, J. (1999) Dimerization of the extracellular domain of the receptor for epidermal growth factor containing the membrane-spanning segment in response to treatment with epidermal growth factor, *J. Biol. Chem.* 274, 35985–35990.
- Ferguson, K. M., Darling, P. J., Mohan, M. J., Macatee, T. L., and Lemmon, M. A. (2000) Extracellular domains drive homo- but not hetero-dimerization of erbB receptors, *EMBO J.* 19, 4632–4643.

43. Garrett, T. P. J., McKern, N. M., Lou, M., Elleman, T. C., Adams, T. E., Lovrecz, G. O., Zhu, H., Walker, F., Frenkel, M. J., Hoyne, P. A., Jorissen, R. N., Nice, E. C., Burgess, A. W., and Ward, C. W. (2002) Crystal structure of a truncated epidermal growth factor receptor extracellular domain bound to transforming growth factor  $\alpha$ , *Cell* 110, 763–773.
44. Burgess, A. W., Cho, H., Eigenbrot, C., Ferguson, K. M., Garrett, T. P. J., Leahy, D. J., Lemmon, M. A., Sliwkowski, M. X., Ward, C. W., and Yokoyama, S. (2003) An open-and-shut case? Recent insights into the activation of EGF/ErbB receptors, *Mol. Cell* 12, 541–552.
45. Riese, D. J., II, and Stern, D. F. (1998) Specificity within the EGF family/ErbB receptor family signaling network, *BioEssays* 20, 41–48.
46. Olayioye, M. A., Neve, R. M., Lane, H. A., and Hynes, N. E. (2000) The ErbB signaling network: Receptor heterodimerization in development and cancer, *EMBO J.* 19, 3159–3167.
47. Ghashghaei, H. T., Weber, J., Pevny, L., Schmid, R., Schwab, M. H., Lloyd, K. C. K., Eisenstat, D. D., Lai, C., and Anton, E. S. (2006) The role of neuregulin-ErbB4 interactions on the proliferation and organization of cells in the subventricular zone, *Proc. Natl. Acad. Sci. U.S.A.* 103, 1930–1935.
48. Jones, F. E., Golding, J. P., and Gassmann, M. (2003) ErbB4 signaling during breast and neural development: Novel genetic models reveal unique ErbB4 activities, *Cell Cycle* 2, 555–559.
49. Yarden, Y., and Sliwkowski, M. X. (2001) Untangling the ErbB signalling network, *Nat. Rev. Mol. Cell Biol.* 2, 127–137.
50. Meert, A., Martin, B., Paesmans, M., Berghmans, T., Mascaux, C., Verdebout, J., Delmotte, P., Lafitte, J., and Sculier, J. (2003) The role of HER-2/neu expression on the survival of patients with lung cancer: A systematic review of the literature, *Br. J. Cancer* 89, 959–965.

BI061436F